

Diffusive Molecular Communication in Biological Cylindrical Environment

Mohammad Zoofaghari, Hamidreza Arjmandi

Department of Electrical Engineering, Yazd University

zoofaghari@yazd.ac.ir, arjmandi@yazd.ac.ir

Abstract—Diffusive molecular communication (DMC) is one of the most promising approaches for realizing nano-scale communications for healthcare applications. In in-vivo environment, DMC system faces bounded biological spaces. Inspired by the blood vessels in the body, a DMC system in a biological cylindrical environment is considered whose boundary is covered by the receptor proteins and information molecules in fluid medium are subject to degradation. Assuming flow with constant velocity, concentration Green's function of diffusion is analytically derived which takes into account asymmetry in all radial, axial and azimuthal coordinates. Employing obtained Green's function, information channel between an arbitrary transmitter and transparent receiver nanomachine is fully characterized. To evaluate the DMC system in the biological cylinder, a simple on-off keying modulation scheme is adopted and corresponding error probability is derived.

Index Terms—Diffusion-based molecular communication (DMC), biological environment, partial differential equation.

I. INTRODUCTION

Diffusion based molecular communication (DMC) is a promising approach for realizing nano communications [1]. In DMC, information is encoded in the concentration, type, and/or release time of molecules. In particular, a transmitter nanomachine releases information molecules into the environment. The released molecules move randomly via Brownian motion and may be observed at the receiver [2]. The Brownian motion of molecules is affected by the environment properties, particularly the geometry of the environment is taken into account through boundary conditions.

Diffusion in an ideal unbounded environment has been extensively studied in MC literature [3]- [11]. Diffusive molecules in an unbounded environment are dispersed in all directions. Thereby, the range of the communication is very limited in unbounded environment. Obtaining a longer range of communication requires high release rate of molecules which may be impossible for nanomachines with constrained resource. Moreover, the unbounded environment is not a realistic assumption for MC applications. For instance, DMC for healthcare applications faces in-vivo environment with biological boundaries.

Inspired by the vessel-like structures in body, a bounded cylindrical environment is a more realistic model which may extend the range of DMC. Investigation of MC in the cylindrical environment with different assumptions has been considered in the literature. In [12] a MC system in confined space of a microfluidic chip is considered to compare different

propagation schemes of free diffusion, and active transport in terms of the achievable rates. The authors characterize communication channel for Brownian motion inside the confined environment with elastic walls by using particle based simulation. In [13], a DMC model is proposed in which a tunnel composed of destroyer molecules exist between the transmitter and receiver to decrease the variance of the hitting times and obtain better signal shape. The hitting times and probabilities are obtained based on simulation results. The response to a pulse of carriers released by a mobile transmitter, measured on a number of receivers located along the vessel wall based on simulation results is studied in [14]. In [15], a tunnel-like environment for DMC is considered where the receiver partially covers the cross-section of the tunnel and tunnel boundaries reflect the molecules upon contact. The distribution of hitting locations is obtained based on simulation results. Papers [12]- [15] characterize MC channel only based on the simulation results without providing mathematical analysis. The authors in [16] consider the diffusion environment as a straight cylindrical duct which is filled with a fluid with steady laminar flow. Assuming a transmitter point source, the channel impulse responses for two simplifying flow regimes called dispersion and flow-dominant are obtained. The authors in [17] consider a 3-D microfluidic channel environment in the presence of flow where the boundaries are reflective. By employing the symmetry in azimuthal coordinate, the authors derive channel impulse response in radial and axial coordinates. The channel impulse response analysis provided in both works [16]- [17] are not able to consider the asymmetry of diffusion in azimuthal coordinate which is required for an arbitrary geometry of transmitter and receiver locations. Moreover, a simple reflective boundary is assumed in both works. This assumption may not be able to apply in in-vivo environments, where biological boundary may be covered by receptor proteins leading to partially reflection-absorbing of molecules. Besides, the effect of degradation mechanism inside the cylindrical environment has not been analyzed in the previous works. Degradation mechanism may be employed to overcome intersymbol interference (ISI) of the diffusion channel [18].

In this paper, we consider a point-to point DMC system in a biological cylindrical environment where the boundary is assumed to be partially reflective-absorbing. A molecule hitting the boundary may be absorbed with a probability and otherwise is reflected. More accurately, we assume the

boundary is covered by the receptor proteins which may react with information molecules hitting the boundary (ligands) and produce the ligand-receptor complexes. Moreover, a degradation reaction is considered within the environment where the diffusive information molecule may be transformed into another type which is modeled as a first order reaction. Assuming flow with constant velocity, concentration Green's function of diffusion is analytically derived in terms of a convergent infinite series which takes into account asymmetry in all radial, axial and azimuthal coordinates. Although, accurate analysis adopts a constant velocity flow, but our results indicate that the proposed analysis well approximates the concentration Green's function in the well-known Poiseuille flow model for enough small effective velocity values. The transmitter and receiver are assumed at arbitrary locations in the described biological cylindrical environment. Employing obtained Green's function, the average received signal at the observer receiver is analytically obtained given an arbitrary transmitted modulated signal (not necessarily impulsive release signal) from an arbitrary transmitter geometry (not necessarily point source). Further, the noise at the receiver due to the randomness of release process at the transmitter, Brownian motion, degradation inside the environment, and binding with receptor proteins over the boundary is analyzed. Thereby, information channel between the transmitter and receiver is fully characterized. To evaluate the proposed DMC system, a simple on-off keying modulation scheme is adopted and corresponding error probability is derived. Our particle based simulation (PBS) results confirm the proposed analysis. In our results, the effects of different system parameters including cylinder radius, flow velocity, degradation inside the environment, and different boundary conditions on the concentration Green's function are examined and discussed.

II. SYSTEM MODEL

A point-to-point DMC system is considered within a cylindrical environment. Cylindrical coordinate system is employed to describe the environment where (ρ, z, φ) denote to radial, axial, and azimuthal coordinates, respectively. An infinite-height cylinder is assumed where the geometric location of points on cylinder is described as

$$\rho = \rho_c. \quad (1)$$

The transmitter is assumed to be a point source located inside the cylinder at an arbitrary point $\bar{r}_{tx} = (\rho_{tx}, z_{tx}, \varphi_{tx})$ where $0 \leq \rho_{tx} \leq \rho_c$. The transmitter uses signaling molecule of type A . A transparent spherical receiver with radius R_{rx} is assumed that does not affect the Brownian motion of molecules whose center is located at $\bar{r}_{rx} = (\rho_{rx}, z_{rx}, \varphi_{rx})$. A schematic illustration of the system model is represented in Fig. 1

The cylinder is filled with a liquid with the diffusion coefficient D (m^2/s) for signaling molecules A which is uniform in all directions. A flow with constant velocity v m/s in axial direction is considered inside the cylinder, i.e., we have $\bar{v}(\bar{r}) = v\hat{a}_z$ m/s . It is assumed the signaling molecules

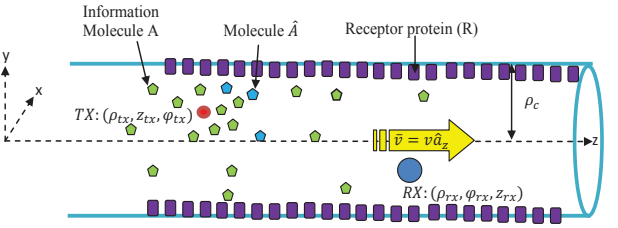


Fig. 1. Schematic illustration of the considered DMC system.

released in the environment may degrade with a probability and transform to another molecule type under the following first order reaction



The boundary is assumed to be covered by protein receptors where hitting molecules (ligands) may react with the protein receptors over the boundary. Depending on the forward reaction rate constant k_2 , this leads to the reflection of the hitting molecule or activation of the receptor and producing the ligand-receptor molecule (AR). We assume the backward reaction rate constant is zero and a molecule that bind to the receptor will not return to the environment. Therefore, we have



It is obvious that the boundary reduces to the pure reflective and absorbing boundary for $k_2 = 0$ and $k_2 = \infty$, respectively.

A time-slotted communication scenario with the time slot duration of T seconds is considered. The transmitter control (modulates) the average release rate of molecules into the environment according to the input symbol. The released molecules diffuse following a Brownian motion and their movements are assumed to be independent of each other. The observer receiver counts the number of molecules fallen inside its volume at a sampling time t_s to decide about the intended transmitted symbol. To evaluate the performance of the system, a simple on-off keying modulation is adopted. Bits 1 and 0 are represented by the instantaneous release of N molecules (on average) and no molecule, respectively. To analyze the presented DMC system, we first characterize the diffusion channel between the transmitter and receiver in the next section.

III. CHARACTERIZING DIFFUSION IN BIOLOGICAL CYLINDRICAL ENVIRONMENT

In this section, we derive concentration Green's function for diffusion inside the cylinder described above.

To this end, we assume the point source transmitter located at $\bar{r}_{tx} = (\rho_{tx}, z_{tx}, \varphi_{tx})$ with instantaneous molecule release

rate $\delta(t - t_0)$ molecule(*mol*)/*s*, where $\delta(\cdot)$ is Dirac delta function. Considering flow with velocity field $\bar{v}(\bar{r}) = v\hat{a}_z$ *m/s* and the degradation mechanism described by (2), the diffusion is described by following equation

$$D\nabla^2C(\bar{r}, t|\bar{r}_{tx}, t_0) - \bar{v}(\bar{r})\cdot\nabla C(\bar{r}, t|\bar{r}_{tx}, t_0) - k_1C(\bar{r}, t|\bar{r}_{tx}, t_0) + S(\bar{r}, t, \bar{r}_{tx}, t_0) = \frac{\partial C(\bar{r}, t|\bar{r}_{tx}, t_0)}{\partial t} \quad (4)$$

where $C(\bar{r}, t|\bar{r}_{tx}, t_0)$ denotes the concentration of molecules at point \bar{r} inside the cylinder and time *t* given the impulsive point source $S(\bar{r}, t, \bar{r}_{tx}, t_0) = \frac{\delta(\rho - \rho_{tx})}{\rho}\delta(\varphi - \varphi_{tx})\delta(z - z_{tx})$. $C(\bar{r}, t|\bar{r}_{tx}, t_0)$ that solves (4) is referred to as concentration Green's function (CGF) of diffusion in the cylinder in the rest of the paper.

Equation (4) in cylindrical coordinate system is simplified as follows

$$D\frac{\partial^2 C(\bar{r}, t|\bar{r}_{tx}, t_0)}{\partial \rho^2} + \frac{D}{\rho}\frac{\partial C(\bar{r}, t|\bar{r}_{tx}, t_0)}{\partial \rho} + \frac{D}{\rho^2}\frac{\partial^2 C(\bar{r}, t|\bar{r}_{tx}, t_0)}{\partial \varphi^2} + D\frac{\partial^2 C(\bar{r}, t|\bar{r}_{tx}, t_0)}{\partial z^2} + v\frac{\partial C(\bar{r}, t|\bar{r}_{tx}, t_0)}{\partial z} - k_1C(\bar{r}, t|\bar{r}_{tx}, t_0) + \frac{\delta(\rho - \rho_{tx})}{\rho}\delta(\varphi - \varphi_{tx})\delta(z - z_{tx})\delta(t - t_0) = \frac{\partial C(\bar{r}, t|\bar{r}_{tx}, t_0)}{\partial t}. \quad (5)$$

The reaction of information molecules with receptors over the cylinder boundary given in (3) is characterized by the third type (Robin) boundary condition as following

$$D\frac{\partial C(\bar{r}, t|\bar{r}_{tx}, t_0)}{\partial \rho} \Big|_{\bar{r}=(\rho_c, z, \varphi)} = k_2C(\bar{r}, t|\bar{r}_{tx}, t_0) \Big|_{\bar{r}=(\rho_c, z, \varphi)}. \quad (6)$$

We have also the implicit axial unbounded conditions that concentration is zero when $z \rightarrow \pm\infty$, i.e.,

$$C(\bar{r}, t|\bar{r}_{tx}, t_0) \Big|_{\bar{r}=(\rho_c, z=\pm\infty, \varphi)} = 0. \quad (7)$$

As shown in [23], CGF could be presented as the product of a one-dimensional and a two-dimensional transient Green's function as

$$C(\bar{r}, t|\bar{r}_{tx}, t_0) = C_{\rho\varphi}(\rho, \varphi, t|\rho_{tx}, \varphi_{tx}, t_0)C_z(z, t|z_{tx}, t_0) \quad (8)$$

where $C_{\rho\varphi}(\rho, \varphi, t|\rho_{tx}, \varphi_{tx}, t_0)$ and $C_z(z, t|z_{tx}, t_0)$ are radial-azimuthal and axial direction Green's functions. Thereby, (5) reduces to two independent equations in terms of $C_{\rho\varphi}(\rho, \varphi, t|\rho_{tx}, \varphi_{tx}, t_0)$ and $C_z(z, t|z_{tx}, t_0)$, as follows

$$D\frac{\partial^2 C_{\rho\varphi}(\rho, \varphi, t|\bar{r}_{tx}, t_0)}{\partial \rho^2} + \frac{D}{\rho}\frac{\partial C_{\rho\varphi}(\rho, \varphi, t|\bar{r}_{tx}, t_0)}{\partial \rho} + \frac{D}{\rho^2}\frac{\partial^2 C_{\rho\varphi}(\rho, \varphi, t|\bar{r}_{tx}, t_0)}{\partial \varphi^2} + \frac{\delta(\rho - \rho_{tx})}{\rho}\delta(\varphi - \varphi_{tx})\delta(t - t_0) = \frac{\partial C_{\rho\varphi}(\rho, \varphi, t|\bar{r}_{tx}, t_0)}{\partial t} \quad (9)$$

$$D\frac{\partial^2 C_z(z, t|z_{tx}, t_0)}{\partial z^2} + v\frac{\partial C_z(z, t|z_{tx}, t_0)}{\partial z} - k_1C_z(z, t|z_{tx}, t_0) + \delta(z - z_{tx})\delta(t - t_0) = \frac{\partial C_z(z, t|z_{tx}, t_0)}{\partial t}. \quad (10)$$

Applying (8) in boundary conditions (6) and (7) results in,

$$D\frac{\partial C_{\rho\varphi}(\rho, \varphi, t|\rho_{tx}, \varphi_{tx}, t_0)}{\partial \rho} \Big|_{\rho=\rho_c} = k_2C_{\rho\varphi}(\rho, \varphi, t|\rho_{tx}, \varphi_{tx}, t_0), \quad (11)$$

and

$$C_z(z, t|z_{tx}, t_0) \Big|_{z=\pm\infty} = 0, \quad (12)$$

respectively. Therefore, $C_{\rho\varphi}(\rho, \varphi, t|\rho_{tx}, \varphi_{tx}, t_0)$ and $C_z(z, t|z_{tx}, t_0)$, can be obtained from (9) subject to the boundary condition (11) and (10) subject to the implicit boundary condition (12). In the following, we present the solutions for these two partial differential equations.

A. Derivation of radial-azimuthal CGF

In this subsection, we solve (9) subject to the boundary condition given in (11). The source term of $\frac{\delta(\rho - \rho_{tx})}{\rho}\delta(\varphi - \varphi_{tx})\delta(t - t_0)$ in (9) is equivalent to an initial condition of

$$C_{\rho\varphi}(\rho, \varphi, t = t_0|\bar{r}_{tx}, t_0) = \frac{\delta(\rho - \rho_{tx})}{\rho}\delta(\varphi - \varphi_{tx}). \quad (13)$$

By considering this initial condition and removing the source term, a homogeneous partial differential equation is obtained which can be solved by technique of separation of variables. Applying $C_{\rho\varphi}(\rho, \varphi, t|\bar{r}_{tx}, t_0) = R(\rho|\rho_{tx})\Phi(\varphi|\varphi_{tx})T(t|t_0)$ in (9) without the source term, dividing both sides by $R(\rho|\rho_{tx})\Phi(\varphi|\varphi_{tx})T(t|t_0)$, and some simple manipulation we have

$$\frac{\rho^2 R''(\rho|\rho_{tx})}{R(\rho|\rho_{tx})} + \frac{\rho R'(\rho|\rho_{tx})}{R(\rho|\rho_{tx})} - \frac{\rho^2 T'(t|t_0)}{DT(t|t_0)} = \frac{\Phi''(\varphi|\varphi_{tx})}{\Phi(\varphi|\varphi_{tx})} \stackrel{a}{=} \alpha \quad (14)$$

where equality with a constant α holds, since we have two separated functions above in left and right hand sides of the first equality. Thereby, we have the following ordinary differential equation

$$\Phi''(\varphi|\varphi_{tx}) - \alpha\Phi(\varphi|\varphi_{tx}) = 0. \quad (15)$$

Considering that the concentration is periodic with period 2π in terms of φ variable and is symmetric versus $\varphi = \varphi_{tx}$, $\alpha = -n^2$, $n \in \{0, 1, \dots\}$ and correspondingly $\Phi_n(\varphi|\varphi_{tx}) = G_n \cos(n(\varphi - \varphi_{tx}))$ is acceptable solution for (15), where G_n is constant.

Considering $\alpha = -n^2$ in (14) and some simple manipulation, we obtain

$$\frac{DR_n''(\rho|\rho_{tx})}{R_n(\rho|\rho_{tx})} + \frac{DR_n'(\rho|\rho_{tx})}{\rho R_n(\rho|\rho_{tx})} + \frac{Dn^2}{\rho^2} = \frac{T_n'(t|t_0)}{T_n(t|t_0)} \stackrel{b}{=} -\gamma_n^2 \forall n \in 0, 1, \dots \quad (16)$$

Note that only a negative constant on the right side is possible, since a positive constant leads to unbounded function $T(t|t_0)$ and correspondingly unbounded concentration function of time. For simplicity we set $\gamma_n = \sqrt{D}\lambda_n$. Thereby, we have the following ordinary differential equation

$$\rho^2 R_n''(\rho|\rho_{tx}) + \rho R_n'(\rho|\rho_{tx}) + (\lambda_{mn}^2 - \frac{n^2}{\rho^2})R_n(\rho|\rho_{tx}) = 0, \quad (17)$$

subject to the following boundary condition obtained from (11)

$$DR_n'(\rho|\rho_{tx})|_{\rho=\rho_c} = k_2R_n(\rho_c|\rho_{tx}). \quad (18)$$

Solution of (17) in general form could be written as

$$R_n(\rho|\rho_{tx}) = A_n J_n(\lambda_n \rho) + B_n Y_n(\lambda_n \rho), \quad (19)$$

where $J_n(\cdot)$ and $Y_n(\cdot)$ are n^{th} order of first and second types of Bessel functions, respectively, for every positive value λ_n . Since $Y_n(\lambda_{mn}\rho)$ is singular at $\rho = 0$, $B_n = 0$. On the other hand, considering (18), each root of the following equation is an acceptable λ_n value.

$$D\lambda_n J_n'(\lambda_n \rho_c) = k_2 J_n(\lambda_n \rho_c). \quad (20)$$

Denoting the the m^{th} root of the above equation, $R_{nm}(\rho_c | \rho_{tx}) = A_{nm} J_n(\lambda_{nm}\rho)$ is a solution for (14) with boundary condition (18). Given λ_n and considering the implicit condition of $T(t \rightarrow \infty | t_0) = T(t | t_0) = I_{nm} e^{-D\lambda_{nm}^2(t-t_0)} u(t-t_0)$ satisfies (16), where I_{nm} is a constant. Therefore, we have

$$C_{\rho\varphi}(\rho, \varphi, t | \bar{r}_{tx}, t_0) = \sum_{n=0}^{\infty} \sum_{m=1}^{\infty} H_{nm} J_n(\lambda_{nm}\rho) \cos(n(\varphi - \varphi_{tx})) e^{-D\lambda_{nm}^2(t-t_0)} u(t-t_0) \quad (21)$$

where $H_{nm} = G_n A_{nm} I_{nm}$ which is unknown and should be determined by applying the initial condition of $C_{\rho\varphi}(\rho, \varphi, t = 0 | \bar{r}_{tx}, t_0) = \frac{\delta(\rho - \rho_{tx})}{\rho} \delta(\varphi - \varphi_{tx})$. Delta functions $\delta(\varphi - \varphi_{tx})$ and $\frac{\delta(\rho - \rho_{tx})}{\rho}$ can be expanded as following, respectively, [24]

$$\delta(\varphi - \varphi_{tx}) = \sum_{n=0}^{\infty} \beta_n \cos(n(\varphi - \varphi_{tx})), \quad (22)$$

where $\beta_0 = \frac{1}{2\pi}$ and $\beta_n = \frac{1}{\pi}$, $n \geq 1$, and

$$\frac{\delta(\rho - \rho_{tx})}{\rho} = \sum_{m=1}^{\infty} \frac{J_n(\lambda_{nm}\rho_{tx})}{N_{nm}} J_n(\lambda_{nm}\rho). \quad (23)$$

in which

$$N_{mn} = \int_0^{\rho_c} \rho J_n^2(\lambda_{mn}\rho) d\rho \quad (24)$$

$$= \frac{\rho_c^2}{2} (J_n^2(\lambda_{mn}\rho_c) - J_{n-1}(\lambda_{mn}\rho_c) J_{n+1}(\lambda_{mn}\rho_c))$$

Employing (21)-(23) in (13) and comparing left and right hand of the equation, we obtain

$$H_{nm} = \frac{J_n(\lambda_{nm}\rho_{tx})}{N_{nm}} \beta_n, \quad n \geq 0, m \geq 1. \quad (25)$$

B. Derivation of axial and final CGF

To solve (10), we take Fourier transform of both sides of (10) in terms of axial variable z and we obtain

$$(-D\beta^2 - k_1 - j\beta v) \tilde{C}_z(\beta, t | z_{tx}, t_0) + \delta(t-t_0) = \frac{\partial \tilde{C}_z(\beta, t | z_{tx}, t_0)}{\partial t}. \quad (26)$$

where $\tilde{C}_z(\beta, t | z_{tx}, t_0)$ denotes the Fourier transform of $C_z(z, t | z_{tx}, t_0)$, i.e., we have

$$C_z(z, t | z_{tx}, t_0) = \frac{1}{2\pi} \int_{-\infty}^{\infty} \tilde{C}_z(\beta, t | z_{tx}, t_0) e^{j\beta z} d\beta. \quad (27)$$

Given β , this is an ODE in terms of t which can be easily solved as

$$\tilde{C}_z(\beta, t | z_{tx}, t_0) = \frac{e^{(-D\beta^2 - k_1 - j\beta v)(t-t_0)}}{2\pi}. \quad (28)$$

By taking the inverse Fourier transform in (27), we obtain

$$C_z(z, t | z_{tx}, t_0) = \frac{1}{\sqrt{(4\pi D(t-t_0))}} e^{\frac{-(z-z_0-v(t-t_0))^2}{4D(t-t_0)} - k_d(t-t_0)} u(t-t_0). \quad (29)$$

Substituting (21) and (29) in (8), the CGF of diffusion in cylinder is obtained as follows

$$C(\bar{r}, t | \bar{r}_{tx}, t_0) = \frac{1}{\sqrt{(4\pi D(t-t_0))}} e^{\frac{-(z-z_0-v(t-t_0))^2}{4D(t-t_0)} - k_d(t-t_0)} \times \sum_{n=0}^{\infty} \sum_{m=1}^{\infty} \frac{J_n(\lambda_{nm}\rho_{tx})}{N_{nm}} J_n(\lambda_{nm}\rho) \cos(n(\varphi - \varphi_{tx})) e^{-D\lambda_{nm}^2(t-t_0)} u(t-t_0). \quad (30)$$

where $\beta_0 = \frac{1}{2\pi}$ and $\beta_n = \frac{1}{\pi}$, $n \geq 1$.

IV. DMC CHANNEL CHARACTRIZATION

As shown in the last section, given an impulsive point source of molecule release $\frac{\delta(\rho - \rho_{tx})}{\rho} \delta(\varphi - \varphi_{tx}) \delta(z - z_{tx})$, the CGF at point $\bar{r} = (\rho, \varphi, z)$, $C(\bar{r}, t | \bar{r}_{tx}, t_0)$ is given by (30). Therefore, given an arbitrary transmitter (molecule release source) of $S(\bar{r}, t)$, $\bar{r} \in \Omega$, the concentration at arbitrary observation point $\bar{r} = (\rho, \varphi, z)$ is obtained as follows

$$\int \int \int_{\Omega} \int_{-\infty}^{+\infty} C(\bar{r}, t | \bar{r}', t') S(\bar{r}', t') dt' \rho' d\rho' dz' d\varphi'. \quad (31)$$

where $C(\bar{r}, t | \bar{r}', t')$ is given by (30).

We note that the differential equation in (5) that introduces the system with point source input at $(\rho_{tx}, \varphi_{tx}, z_{tx})$ and output CGF, $C(\bar{r}, t | \bar{r}_{tx}, t_0)$ is linear time invariant. Therefore, for the special case of point source transmitter located at r_{tx} with molecule release rate of $s(t)$, (31) reduces to $s(t) * C(\bar{r}, t | \bar{r}_{tx}, t_0)$ where $*$ is convolution operator.

A. Stochastic of receiver signal

To analyze the noise in the received signal, we first provide the pdf of the observation time of an individual molecule at the receiver in the following. An impulsive point source, $\frac{1}{\rho} \delta(\rho - \rho_{tx}) \delta(\varphi - \varphi_{tx}) \delta(z - z_{tx}) \delta(t - t_0)$, is equivalent to releasing one molecule at time $t = 0$ and point $\bar{r}_{tx} = (\rho_{tx}, \varphi_{tx}, z_{tx})$. Hence, $C(\bar{r}, t | \bar{r}_{tx}, t_0)$ given in (30) can be interpreted as the probability distribution of presence of molecule at point \bar{r} and time t . Therefore, the probability distribution of observation of the molecule in a transparent receiver at sampling time t is obtained as

$$p_{\text{obs}}(t_s) = \int \int \int_{\Omega_{\text{rx}}} C(\bar{r}, t = t_s | \bar{r}_{tx}, t_0) \rho d\rho \varphi dz, \quad (32)$$

where Ω_{rx} denotes the set of points inside the receiver. Assuming an spherical receiver with very small radius R_{rx} , the concentration variations inside the receiver is negligible and the integral in (32) can be well approximated by $\frac{4\pi}{3} R_{\text{rx}}^3 C(\bar{r}_{\text{rx}}, t = t_s | \bar{r}_{tx}, t_0)$, where \bar{r}_{rx} is the center of the receiver and R_{rx} is the receiver volume. The release rate of a realistic transmitter is stochastic, since chemical reactions involve in the release of molecules that are inherently stochastic. In fact, transmitter can control the average release rate

of molecules. For instance, for ion channel and ion pump biosynthetic modulators proposed in [21], [22], the release rate of molecules has been modeled as a Poisson process $\mathbf{s}(t) \sim \text{Poisson}(s(t))$ where $s(t)$ is the average modulated signal.

Assume the transmitter intends to transmit average modulated signal $s(t)$ for $t \in [0, T]$ corresponding with an intended input symbol. Correspondingly, the release rate of molecules is modeled as Poisson process

$$\mathbf{s}(t) \sim \text{Poisson}(s(t)) \quad (33)$$

Assume the interval $[0, T]$ is divided into partitions of length $\Delta\tau$ where the i th partition is denoted by $[\tau, \tau + \Delta\tau]$, and is tagged by the starting time of the interval, τ . Considering (33), the number of the molecules released during the small time interval, $[\tau, \tau + \Delta\tau]$, is Poisson distributed with mean $s(\tau)\Delta\tau$ for $\tau \in [0, T]$. Because of the thinning property of the Poisson distribution, the number of molecules observed at the receiver at time t , and originating from the molecules released during $[\tau, \tau + \Delta\tau]$, $\mathbf{y}(t|\tau)$, is Poisson distributed with mean $y(t|\tau) = s(\tau)p_{\text{obs}}(t - \tau)\Delta\tau$.

Given two disjoint partitions $[\tau_1, \tau_1 + \Delta\tau]$, $[\tau_2, \tau_2 + \Delta\tau]$, the Poisson RVs $\mathbf{s}(\tau_1)\Delta\tau_1$ and $\mathbf{s}(\tau_2)\Delta\tau_2$ are independent and consequently, $\mathbf{y}(t|\tau_1)$ and $\mathbf{y}(t|\tau_2)$ are independent Poisson RVs. Also, since the summation of independent Poisson RVs is Poisson, the number of the molecules observed at the receiver at time $t \in [0, T]$, $\mathbf{y}(t)$, originating from the molecules released in interval $[0, T]$ follows a Poisson distribution with mean

$$y(t) = \sum_i y(t|\tau) = \sum_{\tau} s(\tau)p_{\text{obs}}(t - \tau)\Delta\tau. \quad (34)$$

For $\Delta\tau \rightarrow 0$, we obtain

$$y(t) = \int_0^T s(\tau)p_{\text{obs}}(t - \tau)d\tau = s(t) * p_{\text{obs}}(t). \quad (35)$$

B. Intersymbol interference (ISI)

We characterized the received signal at the receiver due to transmitted signal in the current time slot, in the last subsection. Now, we explain how the residual ISI from the previous time slots can be incorporated in the receiver output.

Let j denote the time slot number such that $j = 0$ refers to the current time slot $[0, T]$ and $j > 0$ denotes a previous time slot $[-jT, -(j-1)T]$. Assume the average modulated signal in time slot j corresponding with the input symbol for transmission in this time slot is denoted by $s_j(t + jT)$. The number of molecules observed in the current time slot, $j = 0$, at time $t \in [0, T]$, originating from a previously transmitted signal $s_j(t + jT)$ in time slot $j > 0$, $[-jT, (1-j)T]$, is denoted by $\mathbf{I}_j(t)$. Similar to the derivation of the stochastic of

$\mathbf{y}(t)$ above, it is straightforward to show that $\mathbf{I}_j(t)$ is Poisson distributed with mean

$$\begin{aligned} I_j(t) &= \int_{-jT}^{(1-j)T} s_j(\tau + jT)p_{\text{obs}}(t - \tau)d\tau \\ &= \int_0^T s_j(\tau)p_{\text{obs}}(jT + t - \tau)d\tau \\ &= s_j(jT + t) * p_{\text{obs}}(jT + t). \end{aligned} \quad (36)$$

Assume the diffusion channel has memory of length M time slots. The total ISI affecting the receiver output originating from M previously transmitted symbols in the current time slot, \mathbf{I} , is given by

$$\mathbf{I} = \sum_{j=1}^M \mathbf{I}_j, \quad (37)$$

which follows a Poisson distribution since the \mathbf{I}_j are mutually independent Poisson RVs for $j \in \{1, \dots, M\}$. Therefore, given the current transmitted modulated signal, $\mathbf{s}_0(t)$, the receiver output in the current time slot is $\mathbf{y}_O = \mathbf{y} + \mathbf{I}$ which is a Poisson distributed RV with mean

$$\begin{aligned} y_O &= s_0(t) * p_{\text{obs}}(t) \\ &+ \sum_{j=1}^M s_j(jT + t) * p_{\text{obs}}(jT + t) \\ &= \sum_{j=0}^M s_j(jT + t) * p_{\text{obs}}(jT + t). \end{aligned} \quad (38)$$

V. PERFORMANCE ANALYSIS FOR OOK MODULATION

In order to evaluate the DMC system performance based on proposed analysis, a simple on-off keying modulation is adopted where bits 1 and 0 are represented by the average modulated signals $s^1(t) = N\delta(t)$ and $s^0(t) = 0$, respectively. In other words, assuming transmission of bit 1, the transmitter release molecules instantaneously at the beginning of the time slot where the number of released molecules is a Poisson RV with mean N . The transparent receiver counts the number of molecules inside the receiver volume at sampling time t_s (which maximize $p_{\text{obs}}(t)$) in each time slot. The receiver uses the observed sample to decide about the transmitted bit.

From the discussion above, given the transmitted bits $B_j = b_j, j \in \{0, 1, \dots, M\}$, we have

$$\Pr(\mathbf{y}_O = y | b_0, b_1, \dots, b_M) = \frac{e^{-\mathbb{E}(\mathbf{Y}_R | b_0, b_1, \dots, b_M)} (\mathbb{E}(\mathbf{Y}_R | b_0, b_1, \dots, b_M))^y}{y!}, \quad (39)$$

where

$$\mathbb{E}(\mathbf{y}_O | b_0, b_1, \dots, b_M) = \quad (40)$$

$$\sum_{j=0}^M b_j N\delta(jT + t) * p_{\text{obs}}(jT + t) = \quad (41)$$

$$\sum_{j=0}^M b_j N p_{\text{obs}}(jT + t).$$

Since the decoder does not know the the correct values of the previously transmitted bits, i.e., $B_j = b_j, j \in \{1, \dots, M\}$, we suboptimally consider the average values of previous transmitted bits for simplicity of decoder. In other words, the ISI from the previously transmitted symbols is approximated as Poisson RV with mean $\sum_{j=1}^M \frac{1}{2} N p_{\text{obs}}(jT + t)$.

Thereby, we will have

$$\Pr(\mathbf{y}_O = y | b_0) = \frac{e^{-\mathbb{E}(\mathbf{y}_O | b_0)} (\mathbb{E}(\mathbf{y}_O | b_0))^y}{y!}, \quad (42)$$

where

$$\mathbb{E}(\mathbf{y}_O | b_0) = b_0 N p_{\text{obs}}(t) + \sum_{j=1}^M \frac{1}{2} N p_{\text{obs}}(jT + t). \quad (43)$$

Assuming $(B_0 = 1) = \Pr(B_0 = 0) = \frac{1}{2}$, the MAP detector for bit B_0 becomes

$$\hat{B}_0 = \arg \max_{b_0 \in \{0, 1\}} \Pr(\mathbf{y}_O = y | b_0). \quad (44)$$

Simplifying (44) leads to a threshold decision rule based on the receiver output in the current time slot, y , i.e., $\hat{B}_0 = 0$, if $y \leq \text{Thr}$, and $\hat{B}_0 = 1$, if $y > \text{Thr}$, where

$$\text{Thr} = \frac{N p_{\text{obs}}(t_s)}{\ln \left(1 + \frac{N p_{\text{obs}}(t_s)}{\sum_{j=1}^M \frac{1}{2} N p_{\text{obs}}(jT + t_s)} \right)}. \quad (45)$$

The error probability of this detector is given by

$$P_{\text{error}} = \frac{1}{2} (\Pr(E | b_0 = 0) + \Pr(E | b_0 = 1)), \quad (46)$$

where E is an error event, and we have

$$\Pr(E | b_0) = \sum_{\substack{b_0=1 \\ y \leq \text{Thr} \\ b_0=0}} \frac{e^{-\mathbb{E}(\mathbf{y}_O | b_0)} (\mathbb{E}(\mathbf{y}_O | b_0))^y}{y!}. \quad (47)$$

VI. SIMULATION AND NUMERICAL RESULTS

In this section, we examine our proposed analysis for diffusion channel in the cylindrical environment. Moreover, the performance of the point-to-point DMC system over this channel is evaluated.

To confirm the proposed analysis of the CGF, we employ a particle based simulator (PBS). In the PBS, the molecule locations are known and the molecules move independently in the 3-dimensional space. In each dimension (Cartesian coordinates), the displacement of a molecule in Δt seconds is modeled as a Gaussian RV with zero mean and variance $2D\Delta t$. During a Δt seconds, a molecule may be degraded (removed) from the environment with probability of $k_2\Delta t$. If a molecule hits the reflective (absorbing) boundary, the molecule is reflected (absorbed) with probability 1. If a molecule hits the boundary with degradation k_1 (it becomes closer than Δr to the boundary), the molecule is absorbed with probability $k_1\Delta r/D$ and is reflected with probability of $1 - k_1\Delta r/D$. For PBS, we have employed Poiseuille flow model in terms

TABLE I
DMC SYSTEM PARAMETERS USED IN SIMULATIONS

Parameter	Variable	Value
Diffusion coefficient	D	$10^{-9} \text{ m}^2/\text{s}$
Cylinder radius	r_c	$5, 10 \mu\text{m}$
Point source transmitter location	$(\rho_{\text{tx}}, z_{\text{tx}}, \varphi_{\text{tx}})$	$(3\mu\text{m}, 0, 0)$
Degradation reaction constant inside the cylinder	k_2	$0, 20 \text{ 1/s}$
Ligand-receptor reaction constant over the surface	k_1	$0, \infty \text{ m/s}$
Receiver radius	r_R	$0.5 \mu\text{m}$
Number of transmitted molecules '1' for bit	N	5×10^4

of $\bar{v}(\bar{r}) = 2v_{\text{eff}}(1 - \frac{\rho^2}{\rho_c^2})\hat{a}_z \text{ m/s}$. Accordingly, the movement of the molecule at a point with radial ρ due to the flow equals to $2v_{\text{eff}}(1 - \frac{\rho^2}{\rho_c^2})\Delta t$. Although, we assumed a constant flow velocity of $v\hat{a}_z$ to have a tractable analysis, our results indicates that the proposed analysis confirms PBS, when average velocity of $v = \int_0^{\rho_c} 2v_{\text{eff}}(1 - \frac{\rho^2}{\rho_c^2})dr = \frac{4}{3}v_{\text{eff}}$ is adopted in the analysis.

The system parameters adopted for the analytical and simulation are given in Table I.

The point source transmitter is located at $(\rho_{\text{tx}}, z_{\text{tx}}, \varphi_{\text{tx}}) = (3\mu\text{m}, 0, 0)$. Diffusion coefficient is $D = 10^{-9} \text{ m}^2/\text{s}$.

Fig. 2 compares the CGF obtained from our analysis given in (30) and particle based simulator (PBS) for observation points located at $r = 2\mu\text{m}, z = 5\mu\text{m}$ with different azimuthal coordinates $\varphi = 0, \pi/2$, and π . The cylinder with reflecting boundary ($k_1 = 0$) and radius $r_c = 5\mu\text{m}$ is considered. To examine only the effect of azimuthal coordinates in our analysis we have assumed a pure diffusion scenario without flow and degradation, i.e., $v_{\text{eff}} = 0$ and $k_2 = 0$. It is observed that the PBS confirms the proposed analysis which captures concentration variations in azimuthal coordinate in addition to radial and axial coordinates. Also, Fig. 2 depicts the CGF obtained from analysis for observation points with $r = 2\mu\text{m}, z = 10\mu\text{m}$ for different azimuthal coordinates of $\varphi = 0, \pi/2$, and π . Comparing with CGF curves for observation points at $r = 2\mu\text{m}, z = 5\mu\text{m}$, it is deduced that CGF variation in azimuthal coordinate decreases by increasing azimuthal distance between point source and observation point ($|z - z_{\text{Tx}}|$). This occurs because the effect of the axial coordinate on diffusion is dominant for large values of $|z - z_{\text{Tx}}|$ as (30) shows.

Fig. 3 depicts the CGF obtained from the analysis in (30) and the PBS for different cylinder radius values of $r_c = 5, 10$, and $15\mu\text{m}$ when the observation point is located at $(2\mu\text{m}, 5\mu\text{m}, \pi/2)$, $v_{\text{eff}} = 0$, $k_1 = 0$, $k_2 = 0$. It is observed that the PBS confirms the proposed analysis. Fig. 2 show that CGF is significantly amplified by decreasing the radius of the cylinder with reflecting boundary. Thereby, a cylinder environment with smaller radius result in more strong received signals in DMC system and consequently may outperform the DMC system performance.

Fig. 4 compares the CGF obtained from our analysis given in (30) and particle based simulator (PBS) for observation points located at $(2\mu\text{m}, 5\mu\text{m}, \pi/2)$ for different flow effective velocities $v_{\text{eff}} = 0, 50, 100$ and $200 \mu\text{m/s}$. The cylinder with reflecting boundary ($k_1 = 0$), radius $r_c = 5\mu\text{m}$ and $k_1 = 0$ is considered. For PBS the Poiseuille flow model has been simulated, while our analysis adopts the average velocity of $4/3v_{\text{eff}}$. It is observed that the proposed analysis coincides the PBS for zero velocity and well approaches PBS results for enough small effective velocity values.

In Fig. 5, the effect of degradation inside the cylinder ($k_2 = 0, 20$), absorbing ($k_1 \rightarrow \infty$), reflective ($k_1 = 0$), and unbounded ($r_c \rightarrow \infty$) boundaries is examined on CGF. The CGF obtained from our analysis given in (30) and PBS has been depicted for observation points located at $(2\mu\text{m}, 5\mu\text{m}, \pi/2)$ when $r_c = 5\mu\text{m}$, $v_{\text{eff}} = 50\mu\text{m/s}$. In all scenarios PBS confirms the proposed analytic results. It is observed that degradation inside the environment and binding with the receptors over the surface weakens the CGF (correspondingly the gain of the diffusion channel) from one side and shorten the tail of CGF (correspondingly the memory of diffusion channel) from the other side. Therefore, a trade off between the gain and memory of the diffusion channel arises in the presence of degradation. As expected, CGF in unbounded scenario has higher amplitudes compared to the absorbing boundary, since the molecules hitting to the boundary are removed and do not have the chance to return to the environment. On the other hand, it has lower amplitudes compared to the reflective boundary, since the molecules movements are limited within the boundary for reflective scenario which leads to higher concentration inside the cylinder. The performance of DMC systems corresponding to the scenarios in Fig. 5 has been compared adopting a simple on-off keying modulation scheme where 0 and 1 are represented by releasing 0 and $N = 5 \times 10^4$ molecules (on average) by the transmitter. The center of the transparent spherical receiver with radius $r_{\text{Rx}} = 0.5\mu\text{m}$ is located at $(2\mu\text{m}, 5\mu\text{m}, \pi/2)$. The receiver observes the number of molecules inside its volume at sampling time in which observation probability (correspondingly the CGF) is maximized. The receiver uses this observation value to decide about received signal. The error probability of different scenarios obtained from (46) has been depicted versus time slot duration. In all scenarios, the BER is a decreasing function of time slot duration, since for a shorter time slot duration (higher transmission rate), since a larger memory and ISI is encountered. It is also observed that the case (absorbing boundary, $k_2 = 20$) results in a higher and lower BER for $T < 0.08$ and $T > 0.08$ compared to (reflective boundary, $k_2 = 20$), respectively. It reveals the trad off between the gain and memory of the diffusion channel resulted from absorbing boundary mentioned above. In fact, for smaller T values the effect of channel memory is dominant and then absorbing memory case has smaller BER and for higher T values, the effect of channel gain is dominant and then the reflective boundary case outperforms BER.

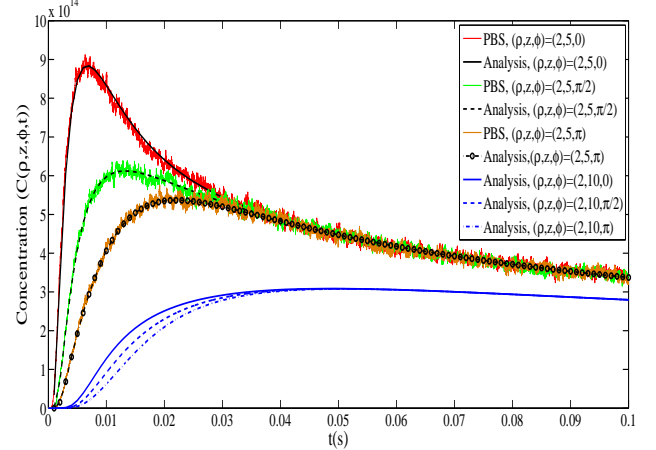


Fig. 2. CGF obtained from analysis and PBS for different locations of observation point.

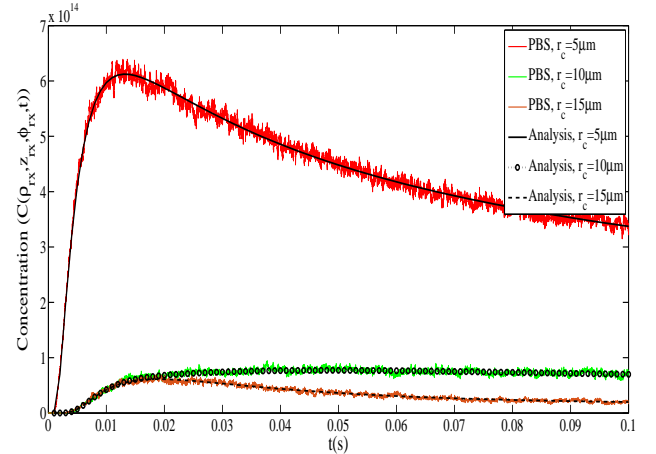


Fig. 3. CGF obtained from analysis and PBS for different cylinder radius, $r_c = 5, 10, 15 \mu\text{m}$.

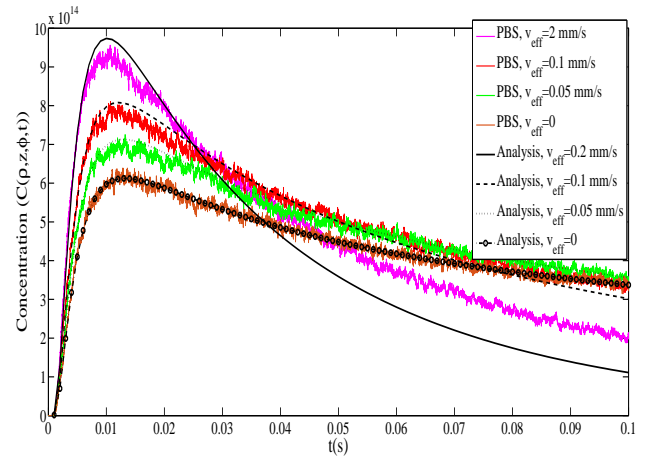


Fig. 4. CGF obtained from analysis and PBS for different flow effective velocities $v_{\text{eff}} = 0, 50, 100$ and $200 \mu\text{m/s}$

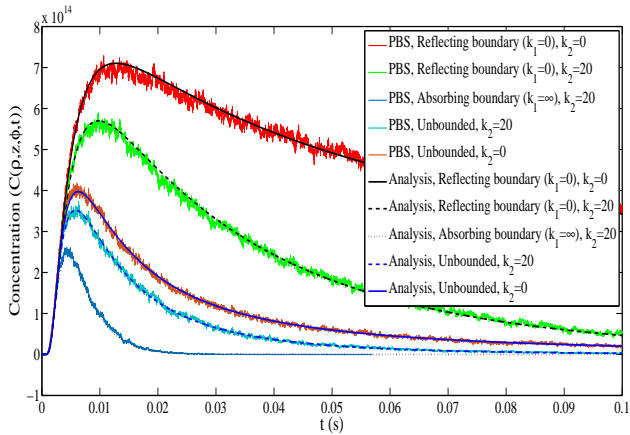


Fig. 5. CGF obtained from analysis and PBS for diffusion in unbounded and cylindrical environment for different k_1 and k_2 values.

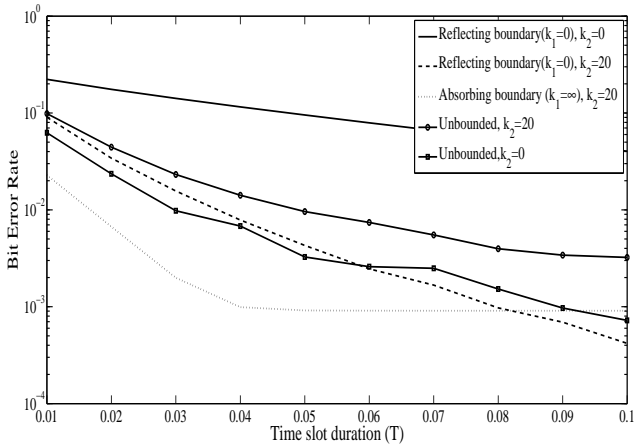


Fig. 6. BER of the DMC system corresponding with scenarios in Fig. 5.

REFERENCES

- [1] Akyildiz, Ian F., Fernando Brunetti, and Cristina Blzquez, "Nanoneetworks: A new communication paradigm," *Computer Networks*, vol. 52, no. 12, pp. 2260-2279, Aug. 2008.
- [2] M. Pierobon and I. Akyildiz, "A physical end-to-end model for molecular communications in nanonetworks," *IEEE Journal on Selected Areas in Communications*, vol. 28, no. 4, pp. 602-611, May 2010.
- [3] M. S. Kuran, H. B. Yilmaz, T. Tugcu, and B. zerman, "Energy model for communication via diffusion in nanonetworks," *Nano Commun. Netw.*, vol. 1, no. 2, pp. 86-95, Jun. 2010.
- [4] M. Pierobon and I. F. Akyildiz, "Diffusion-based noise analysis for molecular communication in nanonetworks," *IEEE Transactions on Signal Processing*, vol. 59, no. 6, pp. 2532-2547, Jun. 2011.
- [5] M. Pierobon and I. F. Akyildiz, "A statistical physical model of interference in diffusion-based molecular nanonetworks," *IEEE Trans. Commun.*, vol. 62, no. 6, pp. 2085-2095, Jun. 2014.
- [6] M. H. Bazargani and D. Arifler, "Deterministic model for pulse amplification in diffusion-based molecular communication," *IEEE Commun. Lett.*, vol. 18, no. 11, pp. 1891-1894, Nov. 2014.
- [7] A. Noel, K. Cheung, and R. Schober, "Optimal receiver design for diffusive molecular communication with flow and additive noise," *IEEE Trans. Nanobiosci.*, vol. 13, no. 3, pp. 350-362, Sep. 2014.
- [8] A. Ajiaz and A. H. Aghvami, "Error performance of diffusion-based molecular communication using pulse-based modulation," *IEEE Trans. Nanobiosci.*, vol. 14, no. 1, pp. 146-151, Jan. 2015.
- [9] D. Kilinc and O. B. Akan, "Receiver design for molecular communication," *IEEE J. Sel. Areas Commun.*, vol. 31, no. 12, pp. 705-714, Dec. 2013.
- [10] X. Wang, M. D. Higgins, and M. S. Leeson, "Relay analysis in molecular communications with time-dependent concentration," *IEEE Commun. Lett.*, vol. 19, no. 11, pp. 1977-1980, Nov. 2015.
- [11] M. U. Mahfuz, D. Makrakis, and H. T. Mouftah, "A comprehensive study of sampling-based optimum signal detection in concentration-encoded molecular communication," *IEEE Trans. Nanobiosci.*, vol. 13, no. 3, pp. 208-222, Sep. 2014.
- [12] Farsad, N., Eckford, A. W., Hiyama, S., Moritani, Y. . On-chip molecular communication: Analysis and design. *IEEE Transactions on NanoBioscience*, vol. 11, no. 3, pp. 304-314, 2012.
- [13] Kuran, M. S., Yilmaz, H. B., Tugcu, T. (2013, June). A tunnel-based approach for signal shaping in molecular communication. In *Communications Workshops (ICC), 2013 IEEE International Conference on* (pp. 776-781). IEEE.
- [14] Felicetti, L., Femminella, M., Reali, G. (2013, July). Establishing digital molecular communications in blood vessels. In *Communications and Networking (BlackSeaCom), 2013 First International Black Sea Conference on* (pp. 54-58). IEEE.
- [15] Turan, M., Kuran, M. S., Yilmaz, H. B., Demirkol, I., Tugcu, T. (2018). Channel Model of Molecular Communication via Diffusion in a Vessel-like Environment Considering a Partially Covering Receiver. *arXiv preprint arXiv:1802.01180*.
- [16] Wicke, Wayan, et al. "Modeling Duct Flow for Molecular Communication." *arXiv preprint arXiv:1711.01479* (2017).
- [17] Dinc, F., Akdeniz, B. C., Pusane, A. E., Tugcu, T. (2018). A General Analytical Solution to Impulse Response of 3-D Microfluidic Channels in Molecular Communication. *arXiv preprint arXiv:1804.10071*.
- [18] A. Noel, K. C. Cheung, and R. Schober, "Improving receiver performance of diffusive molecular communication with enzymes," *IEEE Transactions on NanoBioscience*, vol. 13, no. 1, pp. 31-43, Mar. 2014.
- [19] Al-Zubi, M. M., Mohan, A. S. (2018). Modeling of Ligand-Receptor Protein Interaction in Biodegradable Spherical Bounded Biological Micro-Environments. *IEEE Access*, 6, 25007-25018.
- [20] Dinc, F., Akdeniz, B. C., Pusane, A. E., Tugcu, T. (2018). Impulse Response of the Channel with a Spherical Absorbing Receiver and a Spherical Reflecting Boundary. *arXiv preprint arXiv:1804.03383*.
- [21] H. Arjmandi, A Ahmadzadeh, R. Schober, and M. N. Kenari, "Ion channel based bio-synthetic modulator for diffusive molecular communication," *IEEE Transactions on Nanobioscience*, vol. 15, no. 5, pp. 418-432, Jul. 2016.
- [22] H. Arjmandi, A Ahmadzadeh, R. Schober, and M. N. Kenari, "Ion Pump based bio-synthetic modulator for diffusive molecular communication," *SPAWC 2016* 2016.
- [23] Cole, Kevin D., James V. Beck, A. Haji-Sheikh, and Bahman Litkouhi. *Heat conduction using Greens functions*. CRC Press, 2010.
- [24] Dean G. Duffy. *Green's function with applications*. CRC Press, 2015.
- [25] H. Arjmandi, A. Gohari, M. Nasiri-Kenari, and Farshid Bateni, "Diffusion based nanonetworking: A new modulation technique and performance analysis," *IEEE Communications Letters*, vol. 17, no. 4, pp. 645-648, Apr. 2013.
- [26] G. Aminian, M. Farahnak-Ghazani, M. Mirmohseni, M. Nasiri-Kenari, and F. Fekri, "On the capacity of point-to-point and multiple-access molecular communications with ligand-receptors," *IEEE Transactions on Molecular, Biological and Multi-Scale Communications*, vol. 1, no. 4, pp. 331-346, Dec. 2015.
- [27] R. Mosayebi, H. Arjmandi, A. Gohari, M. Nasiri Kenari, and U. Mitra, "Receivers for diffusion-based molecular communication: Exploiting memory and sampling rate," *IEEE Journal of Selected Areas in Communications*, vol. 32, no. 12, pp. 2368-2380, Dec. 2014.
- [28] L. Felicetti, M. Femminella, G. Reali, T. Nakano, and A. V. Vasilakos, "TCP-like molecular communications," *IEEE Journal on Selected Areas in Communications*, vol. 32, no. 12, pp. 2354-2367, Dec. 2014.